Evidence for nonadiabatic electron-phonon intraband scattering in self-assembled quantum dots

Stefan Menzel, Evgeny A. Zibik,* Pantelis Aivaliotis, John W. Cockburn, and Luke R. Wilson
Department of Physics and Astronomy, University of Sheffield, Sheffield S3 7RH, United Kingdom

Matthew J. Steer
EPSRC National Centre for III-V Technologies, University of Sheffield, Sheffield S1 3JD, United Kingdom
(Received 21 January 2008; published 15 April 2008)

Intraconduction band relaxation in *n*-type InAs/GaAs quantum dots (QDs) for electron transition energies between 124 and 180 meV was investigated by using midinfrared degenerate pump-probe spectroscopy. We find that the intraband electron relaxation after excitation to high energy QD states directly occurs to the QD ground state on a time scale of ~3–10 ps even in the absence of electron-hole scattering. The electron relaxation time exhibits a relatively weak temperature dependence, which is consistent with multiphonon emission induced by nonadiabatic interaction.

DOI: 10.1103/PhysRevB.77.153302 PACS number(s): 78.67.Hc

Enhanced understanding of the electron capture and relaxation processes in self-assembled quantum dots (QDs) is of considerable fundamental interest as well as being essential for improved performance of devices such as high performance lasers[1] and infrared photodetectors.[2] These processes depend on rather complex scattering mechanisms because due to the atomiclike density of states in QDs, conventional electron scattering mechanisms [especially electron longitudinal optical (LO) phonon scattering] are expected to be suppressed in most cases.

Previously, electron scattering mechanisms in QDs were studied by either time resolved photoluminescence[3–5] or nondegenerate pump-probe experiments.[6–8] The majority of the resulting data from these reports suggest intraband relaxation times on a picosecond scale (1–10 ps). This clearly indicates that the early predictions of a "phonon bottleneck"[9] in the conduction band of InAs/GaAs quantum dots are not valid. However, a problem in interpreting the results from such experiments arises from the fact that both techniques generate electron-hole pairs during excitation and, therefore, intraband relaxation can be influenced by interband electron-hole scattering via the Auger-type processes.[10,11]

Moreover, there is an uncertainty concerning the underlying phonon mediated relaxation mechanisms of electrons in excited *p*-, *d*-, and *f*-quantum-dot states. Two possibilities are commonly considered, the first being relaxation in the weak coupling regime. Here, electrons can relax either in a cascaded manner to the QD ground state via intermediate excited states, as suggested by Müller *et al.*,[8] or in one step avoiding intermediate states, as reported by Feldmann *et al.*[12] The second possibility is relaxation in the strong coupling regime between electrons and phonons, wherein polaronic states[13] are formed. In this regime, the phonon bottleneck is removed, allowing picosecond-scale relaxation times with wide transition energy detunings from the phonon energy. Zibik *et al.*[14] reported polaronic relaxation between the QD first excited state and the QD ground state in the conduction band, which arises from polaron decay into longitudinal acoustic phonons on a ~50 ps time scale. For their measurements, they performed degenerate pump-probe experiments by using a free-electron laser in the far infrared. Furthermore, alongside saturation measurements of the QD intraband absorption, Sauvage *et al.*[15] presented a pump-probe measurement of the electron lifetime of ~3 ps at room temperature for a wavelength of ~8 μm. Also, Aivaliotis *et al.*[16] measured an electron relaxation time between the quantum well and QD ground states of ~5 ps for InAs/InGaAs quantum-dot-in-a-well structures. Neither study, however, focused on understanding the underlying relaxation mechanism.

In this Brief Report, we investigate the electron scattering from high energy dot and/or wetting layer (WL) states to the ground state by using degenerate midinfrared pump-probe measurements, in which the electron population is determined only by the doping, giving a more precise control of the QD population compared to interband excitation. Electron-hole scattering is not present with this technique since excitation takes place solely in the conduction band. Very fast intraband relaxation times (3–10 ps) were observed in our sample, which had been doped to one electron per dot. The fast, weakly temperature-dependent relaxation times in our QDs are consistent with a nonadiabatic electron-phonon interaction in QDs, which allows multiphonon assisted carrier relaxation in a wide energy window.

Our QD sample was grown by molecular-beam epitaxy in the Stranski-Krastranow mode on a (100) GaAs substrate with 80 InAs quantum dot layers each separated by a 50 nm GaAs barrier. The average QD density per layer of ~4×10^{10} cm^{-2} was measured prior to the growth of the doped sample by using atomic force microscopy on an uncapped reference sample. The sample was δ doped with Si in the GaAs barriers, 2 nm below the QD layers, and the Si sheet doping density was adjusted to the QD density per layer to obtain a mean occupation of one electron per dot. For the degenerate pump-probe experiments, a femtosecond optical parametric amplifier system (~150 fs pulse width, 1 kHz repetition rate) tunable between 7 and 11 μm (spectral pulse width of ~1 μm) was used. The probe pulses were attenuated with neutral density filters to be about 200 times weaker than the pump pulses, which had an intensity of around 5 MW/cm^2. A photovoltaic liquid nitrogen cooled HgCdTe detector was utilized for detection.

The conduction band transition energies of the sample were measured by using intraband absorption spectroscopy.[17]

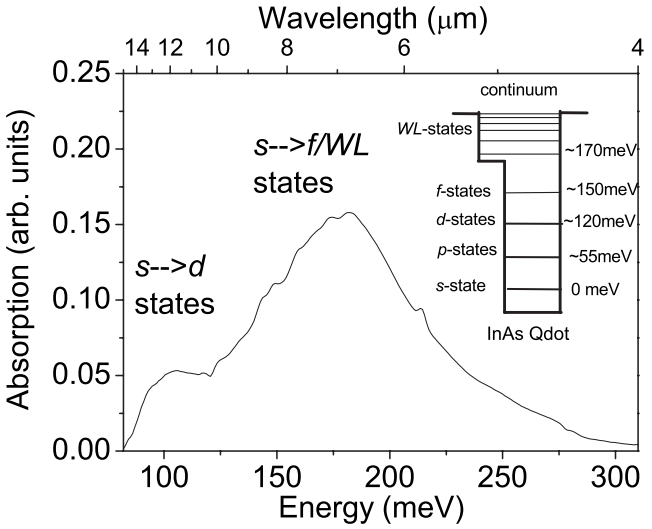

FIG. 1. Intraband absorption of the InAs quantum dot sample at $T=10$ K. The incident light is p polarized (parallel to growth direction). The ground state (s state) is n doped to one electron per dot. The inset shows a drawing of the conduction band structure.

The sample was prepared in a 45° multipass geometry with five reflections to obtain sufficient intraband absorption between the ground state and the high energy QD/WL states, as shown in Fig. 1. The inset shows a diagram of the confined conduction band levels in the InAs quantum dot. The s state (ground state) has been set at $E=0$ and the energetic separation of the p and s states was determined in Ref. 14. The absorption spectrum exhibits a broad peak with a maximum at ~180 meV, which we attribute to electron transitions from the s state to the wetting layer and the f states. In addition, a shoulder is observed at ~110 meV, which we associate with electron transitions from the ground state to the d states.[17]

Having a knowledge of the electronic conduction band transitions allowed us to perform pump-probe experiments. Typical degenerate pump-probe signals are shown in Fig. 2. Displayed are signals at pump-probe energies $E_{pp}=140$ meV and $E_{pp}=180$ meV ($\lambda \sim 9$ μm and ~7 μm), which correspond to an excitation to the quasibound QD/WL states. The signal at $E_{pp}=140$ meV can be fitted by using a single exponential function with a time constant $\tau \sim 4.4 +0.5$ ps. We note that while τ is only a few picoseconds for relaxation from high energy QD states, the relaxation time between the low energy p states and the s state in this sample is much longer [about 50 ps (Ref. 14)]. This suggests that the relaxation from the high energy QD/WL states to the QD ground state bypasses the p states, pointing toward a *direct* relaxation back to the ground state mediated by multiphonon emission.

The transmission recovery signal for the excitation at $E_{pp}=180$ meV has a biexponential time dependence (see inset of Fig. 2) with a short time constant $\tau_1 \sim 8 \pm 1$ ps and a second time constant $\tau_2 \sim 300 \pm 100$ ps. The τ_2 contribution is generally more pronounced for shorter pump-probe wavelengths and vanishes for longer wavelengths. We attribute the initial short decay time to relaxation from excited states directly to the ground state, whereas the longer decay indicates

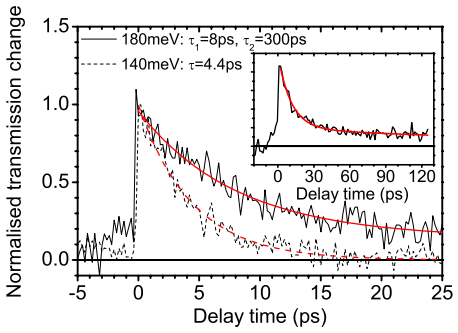

FIG. 2. (Color online) Degenerate pump-probe signals at two different transition energies and $T=10$ K. The inset shows the signal at an energy of 180 meV on a larger scale.

a slow thermal reemission and/or tunneling followed by electron capture to the adjacent trap states.[18] It is not possible to determine the nature of the trap states from our measurements; however, they may be adjacent dots, defects, or deep levels in the barriers. In all of these cases, electrons would be able to escape if excited close to the wetting layer and be captured to these states before relaxing back to the ground state, causing the long decay. It is also important to mention that the strength of our pump-probe signal follows the absorption peak from Fig. 1. Therefore, we can exclude other origins of our pump-probe signal than the intrinsic QD transitions. Furthermore, the variation in the pump power density did not affect the pump-probe signal, indicating that electron-electron scattering plays only a negligible part in this experiment.

In order to identify the electron relaxation and/or capture mechanisms, we have carried out temperature-dependent measurements. The temperature dependence of the relaxation rate at $E_{pp}=124$ meV ($\lambda=10$ μm) is depicted in Fig. 3. Since the pump-probe results indicate that the relaxation of electrons from the excited states directly occurs to the ground state, energy conservation (in the adiabatic approximation) dictates that n LO phonons and m LA phonons must be emitted. The temperature dependence fit function to the

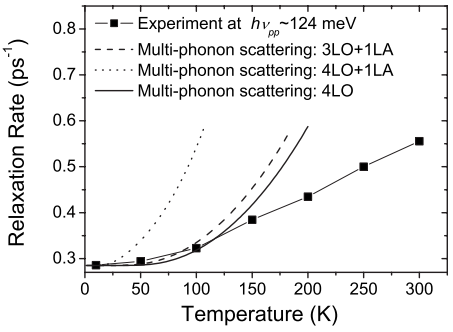

FIG. 3. Relaxation times at a pump-probe energy of around 124 meV and multiphonon (nLO+mLA) scattering fits. Uncertainties in the value for the LO-phonon energy lead to several possible combinations of m and n. Fittings for adiabatic scattering involving combinations of 3 LO (34 meV)+1 LA (20 meV) phonons, 4 LO (29 meV)+1 LA (8 meV) phonons and 4 LO (31 meV) phonons are shown. The experimental data deviate from the fittings because of the weak temperature dependence.

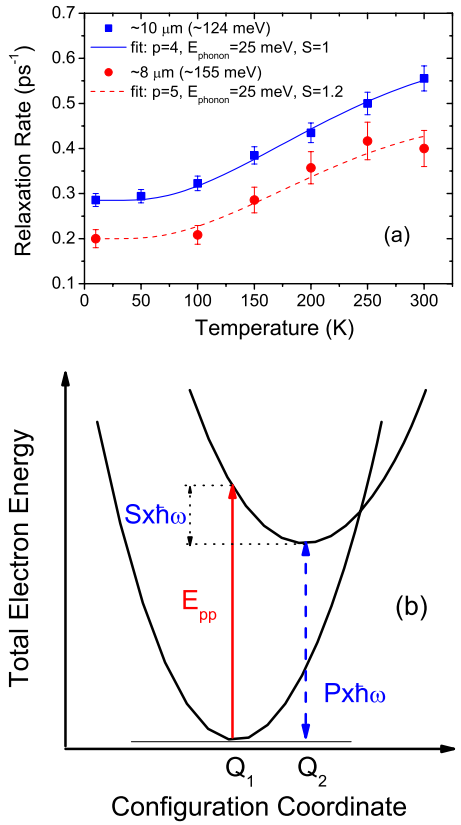

FIG. 4. (Color online) (a) Temperature dependence of the intraband relaxation rate at different pump-probe energies with nonadiabatic multiphonon scattering fit. (b) Energy diagram of the electron energies as a function of the configuration coordinates, which represent the lattice displacement in the event of nonadiabatic scattering.

relaxation rate (Γ), as derived from Fermi's golden rule, is then[8,19]

$$\Gamma = \Gamma_0[N_{\mathrm{LO}}(T)+1]^n[N_{\mathrm{LA}}(T)+1]^m, \tag{1}$$

$$N_{\mathrm{LO/LA}} = \frac{1}{e^{E_{\mathrm{LO/LA}}/kT}-1}, \tag{2}$$

where Γ_0 is the scattering rate at $T=0$ K. Here, $N_{\mathrm{LO/LA}}$ is the Bose-Einstein distribution function for LO and LA phonons. The calculated temperature dependence of Γ for various possible values of n and m that satisfy energy conservation is shown in Fig. 3. Clearly, there is a strong discrepancy between the fit and experimental data, with the latter showing a much weaker temperature dependence.

The temperature dependence of our relaxation times, on the other hand, very well fits to nonadiabatic multiphonon relaxation,[20] as shown in Fig. 4(a). This formalism differs from adiabatic relaxation because it does not treat the electron motion separately (decoupled) from the ion motion in the crystal Hamiltonian. Therefore, the total electron energy and the electron wave functions depend on the lattice displacement, which are expanded in terms of the dimensionless factor Q_i (configuration coordinate) and are shown in Fig. 4(b). This theory is applicable to strongly localized electron wave functions as, e.g., in quantum dots[21] or defects.[22] The strong localization of the wave functions leads to very efficient multiphonon emission which is treated within the Huang-Rhys formalism.[20]

The scattering rates in the nonadiabatic case are derived in a similar manner as in the adiabatic case by using Fermi's golden rule. The difference lies in the Hamiltonian used and the corresponding wave functions, which do not include the simplification (decoupling of lattice and electronic wave functions) introduced by the adiabatic approximation. This full treatment of the scattering leads to complex calculations, as described in Ref. 20. The main parameters involved are the Huang-Rhys parameter S, which describes the electron-phonon coupling strength, and the number of emitted phonons P during the electron relaxation. The resulting equation in the case and/or limit of relatively weak coupling and low temperatures, when the condition $(P+4)^2 \gg 4S^2N(N+1)$ is mathematically satisfied, can be written as

$$\boldsymbol{\Gamma} = \boldsymbol{\Gamma}_0(\mathbf{1}+\boldsymbol{N})^P \boldsymbol{e}^{-2SN}, \tag{3}$$

where Γ_0 is the relaxation rate at $T=0$ K and N represents again the Bose-Einstein distribution function as in Eq. (2). This expression gives very good agreement with our experimental data because it displays a relatively weak temperature dependence. The best fit is obtained for the Huang-Rhys parameters of $S \approx 1$ and $S \approx 1.2$ for the excitations at $E_{\mathrm{pp}}=124$ meV and $E_{\mathrm{pp}}=155$ meV, respectively. A phonon energy of about $\hbar\omega \approx 25$ meV is deduced for both cases with $P=4$ and $P=5$ for the excitation at $E_{\mathrm{pp}}=124$ meV and $E_{\mathrm{pp}}=155$ meV. The phonon energy extracted from these fittings is close to the InAs-like LO-phonon energy in self-assembled InAs QDs, typically within the range of 28–30 meV (interface and bulk).[23] The energy conservation condition in case of nonadiabatic electron-phonon interaction is $E_{\mathrm{pp}}=(S+P)\hbar\omega$.

The above Huang-Rhys parameters are smaller compared to the ones estimated in Ref. 21 (S between 6 and 10) for PbSe nanocrystals. This is to be expected, since it is well known that the electron-phonon interaction strength in II-VI material systems[24,25] is much larger compared to that in III-V systems due to the higher ionicity of the former. Nevertheless, the values of the Huang-Rhys parameters found here are much larger than in bulk materials[26] and for excitonic transitions (typically $\ll 1$) (Ref. 27) because of the Huang-Rhys parameter dependence on the localization size. Our quantum dots are lens shaped and have typical sizes of about 25 nm diameter in QD plane and ~ 3 nm height. S increases with decreasing dot size either as $1/R$ or $1/R^3$ due to stronger localized electron wave functions.[20] Higher energy excited states originate due mainly to confinement in the growth directions with the localization size of ~ 3 nm in our QDs, which is about ten times smaller than the localization in the lateral direction. This can explain why the nonadiabatic electron-phonon interaction governing the relaxation for electron high energy transitions is not significant for s to p transitions. In the latter, the quantization occurs due to electron confinement in lateral direction, thus the electron-

phonon coupling strength is similar to its bulk value and the relaxation of excitation occurs via polaron disintegration.[14]

In conclusion, we have investigated the electron relaxation in *n*-type InAs/GaAs quantum dots by using midinfrared femtosecond pump-probe spectroscopy. This technique allows electron relaxation to be studied in the absence of electron-hole scattering because excitation takes place only in the conduction band. Furthermore, electron-electron scattering is negligible because of the low doping (one electron per dot) in our sample. In spite of the absence of carrier-carrier scattering, we observe the relaxation times in the picosecond range (3–10 ps). Varying the excitation wavelength shows an increase in the relaxation time for excitation to higher energy levels as expected. The temperature dependence of the relaxation time reveals a slow increase toward $T=10$ K and fits well to nonadiabatic relaxation described by the Huang-Rhys formalism.

This work is supported by the European Commission Marie Curie Research Training Network "POISE" and by the Engineering and Physical Sciences Research Council (EPSRC-GB), United Kingdom.

*e.zibik@shef.ac.uk

[1] D. Bimberg, M. Grundmann, F. Heinrichsdorff, N. N. Ledentsov, V. M. Ustinov, A. E. Zhukov, A. R. Kovsh, M. V. Maximov, Y. M. Shernyakov, B. V. Volovik, A. F. Tsatsul'nikov, P. S. Kop'ev, and Z. I. Alferov, Thin Solid Films **367**, 235 (2000).
[2] H. Lim, B. Movaghar, S. Tsao, M. Taguchi, W. Zhang, A. A. Quivy, and M. Razeghi, Phys. Rev. B **74**, 205321 (2006).
[3] J. Siegert, S. Marcinkevicius, and Q. X. Zhao, Phys. Rev. B **72**, 085316 (2005).
[4] K. Gündoğdu, K. C. Hall, Thomas F. Boggess, D. G. Deppe, and O. B. Shchekin, Appl. Phys. Lett. **85**, 4570 (2004).
[5] B. Ohnesorge, M. Albrecht, J. Oshinowo, A. Forchel, and Y. Arakawa, Phys. Rev. B **54**, 11532 (1996).
[6] T. S. Sosnowski, T. B. Norris, H. Jiang, J. Singh, K. Kamath, and P. Bhattacharya, Phys. Rev. B **57**, R9423 (1998).
[7] S. Trumm, M. Wesseli, H. J. Krenner, D. Schuh, M. Bichler, J. J. Finley, and M. Betz, Appl. Phys. Lett. **87**, 153113 (2005).
[8] T. Müller, F. F. Schrey, G. Strasser, and K. Unterrainer, Appl. Phys. Lett. **83**, 3572 (2003).
[9] U. Bockelmann and G. Bastard, Phys. Rev. B **42**, 8947 (1990).
[10] A. V. Uskov, F. Adler, H. Schweizer, and M. H. Pilkuhn, J. Appl. Phys. **81**, 7895 (1997).
[11] G. A. Narvaez, G. Bester, and A. Zunger, Phys. Rev. B **74**, 075403 (2006).
[12] J. Feldmann, S. T. Cundiff, M. Arzberger, G. Böhm, and G. Abstreiter, J. Appl. Phys. **89**, 1180 (2001).
[13] S. Hameau, J. N. Isaia, Y. Guldner, E. Deleporte, O. Verzelen, R. Ferreira, G. Bastard, J. Zeman, and J. M. Gérard, Phys. Rev. B **65**, 085316 (2002).
[14] E. A. Zibik, L. R. Wilson, R. P. Green, G. Bastard, R. Ferreira, P. J. Phillips, D. A. Carder, J.-P. R. Wells, J. W. Cockburn, M. S. Skolnick, M. J. Steer, and M. Hopkinson, Phys. Rev. B **70**, 161305(R) (2004).
[15] S. Sauvage, P. Boucaud, F. Glotin, R. Prazeres, J.-M. Ortega, A. Lemaitre, J.-M. Gérard, and V. Thierry-Flieg, Appl. Phys. Lett. **73**, 3818 (1998).
[16] P. Aivaliotis, S. Menzel, E. A. Zibik, J. W. Cockburn, L. R. Wilson, and M. Hopkinson, Appl. Phys. Lett. **91**, 253502 (2007).
[17] E. A. Zibik, A. D. Andreev, L. R. Wilson, M. J. Steer, R. P. Green, W. H. Ng, J. W. Cockburn, M. S. Skolnick, and M. Hopkinson, Physica E (Amsterdam) **26**, 105 (2005).
[18] Independently, lateral photocurrent measurements have been performed, showing that the wavelength onset of the long component coincides with the photocurrent onset.
[19] T. Inoshita and H. Sakaki, Phys. Rev. B **46**, 7260 (1992).
[20] B. K. Ridley, *Quantum Processes in Semiconductors* (Claredon, Oxford, 1999).
[21] R. D. Schaller, J. M. Pietryga, S. V. Goupalov, M. A. Petruska, S. A. Ivanov, and V. I. Klimov, Phys. Rev. Lett. **95**, 196401 (2005).
[22] P. C. Sercel, Phys. Rev. B **51**, 14532 (1995).
[23] A. G. Milekhin, A. I. Toropov, A. K. Bakarov, D. A. Tenne, G. Zanelatto, J. C. Galzerani, S. Schulze, and D. R. T. Zahn, Phys. Rev. B **70**, 085314 (2004).
[24] R. Akimoto, K. Akita, F. Sasaki, and S. Kobayashi, Appl. Phys. Lett. **80**, 2433 (2002).
[25] B. K. Ridley, Phys. Rev. B **39**, 5282 (1989).
[26] X.-Q. Li and Y. Arakawa, Phys. Rev. B **56**, 10423 (1997).
[27] M. Bissiri, G. B. von Högersthal, A. S. Bhatti, M. Capizzi, A. Frova, P. Frigeri, and S. Franchi, Phys. Rev. B **62**, 4642 (2000).